Preprints of the 19th World Congress
The International Federation of Automatic Control
Cape Town, South Africa. August 24-29, 2014

Artificial Pancreas Systems: An Integrated Multivariable Adaptive Approach

Kamuran Turksoy [*] **Lauretta T. Quinn** [**]
Elizabeth Littlejohn [***] **Ali Cinar** [*,****]

[*] *Biomedical Engineering, Illinois Institute of Technology Chicago, IL 60616 USA (e-mail: kturksoy@hawk.iit.edu).*
[**] *College of Nursing, University of Illinois Chicago, Chicago, IL 60612, USA (e-mail: lquinn1@uic.edu)*
[***] *Biological Sciences Division, University of Chicago, Chicago, IL 60637, USA. (e-mail: elittlej@peds.bsd.uchicago.edu)*
[****] *Chemical and Biological Engineering Department, Illinois Institute of Technology, Chicago, IL 60616, USA. (e-mail: cinar@iit.edu)*

Abstract: An artificial pancreas (AP) system with a hypoglycemia early alarm system and adaptive control system based on multivariable recursive time series models is developed. The inputs of the model include glucose concentration (GC) and physiological signals that provide information about the physical activities and stress of the patient. The stability of the recursive time-series models is guaranteed by a constrained optimization method. Generalized predictive control (GPC) is used to regulate GC. Experiments in a clinical setting illustrate the performance of the AP and compare it to open-loop regulation by the patient. Results show that the AP can regulate GC successfully and prevent hypoglycemia in spite of exercise.

Keywords: Type 1 Diabetes, Artificial Pancreas, Adaptive Control, Hypoglycemia Alarm, Integrated Systems

1. INTRODUCTION

Artificial pancreas systems enable automatic control of blood glucose concentrations (GC) of patients with Type 1 Diabetes (T1D) by providing substitute endocrine functionality of a healthy pancreas. Patients with T1D administer 3-5 insulin injections (usually pre-meal) per day or use a manual insulin pump to keep their GC in normal range (70-180 mg/dl). The success of maintaining GC in normal range by manual injection therapies has been limited. Changing life style conditions such as stress, illness, or physical activity are some factors that affect the performance of manual regulation. Diabetes can cause long-term complications such as cardiovascular diseases, kidney failure, retinopathy, neuropathy, and problems with wound healing. Diabetes has been reported as the seventh leading cause of death in the United States, and the total cost of diagnosed diabetes has been estimated to be $245 billion in 2012 (American Diabetes Association, 2013). Better regulation of GC will reduce the morbidity caused by diabetes and its complications, and medical expenditures.

Use of proportional-integral-derivative (PID) controllers for implementing an artificial pancreas showed the advantages of closed-loop control (Bequette, 2005) but the mean GC remained similar in open-loop and PID closed-loop control which also caused hypoglycemia 2-3 hours post meals (Steil et al., 2006). Model-based control strategies provided better performance by handling delays in GC measurement and insulin delivery and constraints on input and output signals. Model-predictive controllers (MPC) used in vivo (Bruttomesso et al., 2009; Clarke et al., 2009; Breton et al., 2012) needed modification of model parameters for different patients in these studies. Meal information (time and amount) was provided as known disturbances. Adaptive control strategies based on generalized predictive control (GPC) were also proposed (Turksoy et al., 2013a; El-Khatib et al., 2010). Recursive least square (RLS) parameter estimation was used to identify unknown parameters of time-series models in (Turksoy et al., 2013a; El-Khatib et al., 2010) without providing any information about meals. Glucagon was used as a second manipulated variable with a proportional-derivative controller to prevent hypoglycemia events (El-Khatib et al., 2010).

Recursive time-series models are a powerful tool for describing the dynamics of GC (Turksoy et al., 2013a; El-Khatib et al., 2010) and for glucose prediction and hypoglycemia alarm systems (Turksoy et al., 2013b; Eren-Oruklu et al., 2012; Sparacino et al., 2007). Any unconstrained identification method may give unstable models because of process and measurement noise even when the process is known to be stable. Systems such as GC are sensitive to disturbances such as meals and physical activities. Thus it is possible to identify unstable models describing GC dynamics with regular identification methods (RLS, extended least square (ELS) method, and subspace identification), compromising controller or hypoglycemia alarm system performance by using predictions from an unstable model.

Fear of hypoglycemia is a major concern of patients in using AP systems. Many closed-loop studies with various

control algorithms have resulted in mild or severe hypoglycemic episodes (Steil et al., 2006; Schaller et al., 2006; Bruttomesso et al., 2009; Clarke et al., 2009). Mathematical models for the prediction of plasma insulin levels have been incorporated into closed-loop studies for hypoglycemia prevention (Steil et al., 2011; Ruiz et al., 2012; El-Khatib et al., 2010; Turksoy et al., 2013a). Hypoglycemia prediction-based pump suspension methods have been noted to decrease the occurrence of hypoglycemia (Buckingham et al., 2009; Elleri et al., 2010). Bihormonal closed-loop studies (El-Khatib et al., 2010; Ward et al., 2011) using glucagon and insulin have also been proposed for hypoglycemia prevention. Semi-automated hybrid systems (Steil et al., 2011; Weinzimer et al., 2008; Elleri et al., 2013; Breton et al., 2012) have been reported to reduce the increase in postprandial glucose levels and subsequently decrease insulin-induced postprandial hypoglycemia. Although the reported methods decreased the time spent in hypoglycemia, complete avoidance of hypoglycemia was not achieved, and additional carbohydrate (CHO) supplements were needed for treatment of some of hypoglycemic episodes.

An integrated AP with a hypoglycemia early alarm (HEA) system and GPC based control system is reported in this paper. Both systems rely on multivariable recursive time series models developed by extending RLS methods with a constrained optimization method that guarantees model stability. Modifications are made to classical GPC. Physiological signals collected from a sports armband are used to improve the prediction of GC (Eren-Oruklu et al., 2012) and to indicate exercise or sleep to the controller for computing the appropriate insulin infusion rate. Section 2 describes system identification. The HEA system and the GPC system are introduced in Sections 3 and 4. The results comparing the open-loop and closed loop insulin regulation of one subject in a clinical study is presented in Section 5. Discussion and conclusions are given in Sections 6 and 7.

2. SYSTEM IDENTIFICTION

2.1 Recursive Time-Series Models

Recursive time-series models can describe the time-varying dynamics of blood GC (BGC) by adapting the model with every new measurement. An autoregressive moving average model with exogenous inputs (ARMAX) is used to describe BGC dynamics. ARMAX models can easily be extended to multi-input-multi-output systems. An ARMAX model is:

$$A(q^{-1})y(k) = B_i(q^{-1})u_i(k-1-d_i) + C(q^{-1})\epsilon(k) \quad (1)$$

where $y(k)$ is the observation (system output) at time k, $u_i(k-1)$ the i^{th} input, $\epsilon(k)$ white noise, d_i the delay term for input i.

$$A(q^{-1}) = 1 + a_1q^{-1} + a_2q^{-2} + ... + a_{n_A}q^{-n_A} \quad (2)$$

$$B_i(q^{-1}) = b_{0_i} + b_{1_i}q^{-1} + b_{2_i}q^{-2} + ... + b_{n_{B_i}}q^{-n_{B_i}} \quad (3)$$

$$C(q^{-1}) = 1 + c_1q^{-1} + c_2q^{-2} + ... + c_{n_C}q^{-n_C} \quad (4)$$

where q^{-1} is the backward shift operator, and n_A, n_{B_i}, n_C are model orders to be determined from data. Writing the ARMAX model in linear regression form:

$$\hat{y}(k) = \phi(k)^T\hat{\theta}(k) \quad (5)$$

$$\begin{aligned}\phi(k) = [&-y(k-1) \cdots -y(k-n_A) \;\; u_1(k-1-d_1), \\ &\cdots u_1(k-n_{B_1}-d_1) \cdots u_m(k-1-d_m), \\ &\cdots u_m(k-n_{B_m}-d_m) \;\; e(k-1) \cdots e(k-n_C)]^T\end{aligned} \quad (6)$$

$$\begin{aligned}\hat{\theta}(k) = [&a_1 \;\; \cdots \;\; a_{n_A} \;\; b_{0_1} \;\; \cdots \; b_{n_{B_1}} \\ &\cdots \qquad b_{0_m} \;\; \cdots \; b_{nB_m} \;\; c_1 \;\; \cdots \;\; c_{n_C}]^T\end{aligned} \quad (7)$$

where $\phi(k)$ and $\hat{\theta}(k)$ are the vectors of past observations and model parameters, respectively. The white noise term in Eq (6) is replaced with model error $e(k)$ since the former is an unknown signal:

$$e(k) = y(k) - \hat{y}(k) = y(k) - \phi(k)^T\hat{\theta}(k) \quad (8)$$

The coefficients in Eqs (1)-(4) are recomputed with every new measurement and the model is used until the next measurement.

2.2 State Space Representation of RLS

Recursive least square (RLS) parameter estimation is used to identify the unknowns in Eq (7). When the disturbance acting on the system is non-stationary, RLS may estimate coefficients that are outside the stability region. A constrained RLS method must be used to guarantee model stability. To apply the stability constraints to RLS, the time series model is written in state space form.

$$\begin{aligned}X(k) &= \tilde{A}X(k-1) + \tilde{B}\tilde{u}(k-1) + \tilde{K}e(k) \\ y(k) &= \tilde{C}X(k-1) + \tilde{D}\tilde{u}(k-1) + e(k)\end{aligned} \quad (9)$$

with the state matrix $\tilde{A}$

$$\tilde{A} = \begin{bmatrix} -[a_1 \cdots a_{n_A}] & [b_{1_1} \cdots b_{B_1}] & \cdots & [b_{1_m} \cdots b_{B_m}] & [c_1 \cdots c_{n_C}] \\ I_{p\times p} \;\; 0_{p\times 1} & 0_{p\times r_1} \;\; 0_{p\times 1} & \cdots & 0_{p\times r_m} \;\; 0_{p\times 1} & 0_{p\times s} \;\; 0_{p\times 1} \\ 0_{1\times p} \;\; 0 & 0_{1\times r1} \;\; 0 & \cdots & 0_{1\times r_m} \;\; 0 & 0_{1\times s} \;\; 0 \\ 0_{r_1\times p} \;\; 0_{r_1\times 1} & I_{r_1\times r_1} \;\; 0_{r_1\times 1} & \cdots & 0_{r_1\times r_m} \;\; 0_{r_1\times 1} & 0_{r_1\times s} \;\; 0_{r_1\times 1} \\ \vdots \;\; \vdots & \vdots \;\; \vdots & \cdots & \vdots \;\; \vdots & \vdots \;\; \vdots \\ 0_{1\times p} \;\; 0 & 0_{1\times r1} \;\; 0 & \cdots & 0_{1\times r_m} \;\; 0 & 0_{1\times s} \;\; 0 \\ 0_{r_m\times p} \;\; 0_{r_m\times 1} & 0_{r_m\times r_1} \;\; 0_{r_m\times 1} & \cdots & I_{r_m\times r_m} \;\; 0_{r_m\times 1} & 0_{r_m\times s} \;\; 0_{r_m\times 1} \\ 0_{s\times p} \;\; 0_{s\times 1} & 0_{s\times r_1} \;\; 0_{s\times 1} & \cdots & 0_{s\times r_m} \;\; 0_{s\times 1} & I_{s\times s} \;\; 0_{s\times 1} \end{bmatrix} \quad (10)$$

where $p = n_A - 1$, $r_i = n_{B_i} - 2$ (for $i = 1, \cdots, m$) and $s = n_C - 1$

$$X(k-1) = \begin{bmatrix} \begin{bmatrix} y(k-1) \\ y(k-2) \\ \vdots \\ y(k-n_A) \end{bmatrix} \\ \begin{bmatrix} u_1(k-1-1) \\ u_1(k-1-2) \\ \vdots \\ u_1(k-1-n_{B_1}) \end{bmatrix} \\ \vdots \\ \begin{bmatrix} u_m(k-1-1) \\ u_m(k-1-2) \\ \vdots \\ u_m(k-1-n_{B_m}) \end{bmatrix} \\ \begin{bmatrix} e(k-1) \\ e(k-2) \\ \vdots \\ e(k-n_C) \end{bmatrix} \end{bmatrix} \quad \tilde{B} = \begin{bmatrix} b_{0_1} & \cdots & b_{0_m} \\ 0 \;\; 0_{1\times(m-2)} & & 0 \\ \vdots & \vdots & \vdots \\ 0 \;\; 0_{1\times(m-2)} & & 0 \\ 1 \;\; 0_{1\times(m-2)} & & 0 \\ 0 \;\; 0_{1\times(m-2)} & & 0 \\ \vdots & \vdots & \vdots \\ 0 \;\; 0_{1\times(m-2)} & & 0 \\ \vdots & \vdots & \vdots \\ 0 \;\; 0_{1\times(m-2)} & & 1 \\ 0 \;\; 0_{1\times(m-2)} & & 0 \\ \vdots & \vdots & \vdots \\ 0 \;\; 0_{1\times(m-2)} & & 0 \\ 0 \;\; 0_{1\times(m-2)} & & 0 \\ 0 \;\; 0_{1\times(m-2)} & & 0 \\ \vdots & \vdots & \vdots \\ 0 \;\; 0_{1\times(m-2)} & & 0 \end{bmatrix} \quad (11)$$

$$\tilde{D} = [\, b_{0_1} \;\cdots\; b_{0_m} \,] \;\; \tilde{u}\,(k-1) = \begin{bmatrix} u_1(k-1) \\ \vdots \\ u_m(k-1) \end{bmatrix} \quad (12)$$

$$\tilde{C} = [\,-[a_1 \cdots a_{n_A}]\ [b_{1_1} \cdots b_{B_1}] \cdots [b_{1_m} \cdots b_{B_m}]\ [c_1 \cdots c_{n_C}]\,] \quad (13)$$

$$\tilde{K} = [\,1\ 0 \cdots 0\ 0\ 0 \cdots 0 \cdots 0\ 0 \cdots 0\ 1\ 0 \cdots 0\,]^T \quad (14)$$

2.3 Constrained Recursive Least Squares

RLS can be extended to weighted RLS (WRLS) in order to assign different importance to specific measured values over time. The coefficients of the ARMAX model are obtained by minimizing the constrained objective function:

$$\begin{aligned} \hat{\theta}(k) = \min_{\theta(k)} [\Delta\theta^T P^{-1}(k-1)\Delta\theta + e(k)^2] \\ s.t.\ \rho(\tilde{A}) \leq 1 \\ \theta_{min} \leq \theta(k) \leq \theta_{max} \end{aligned} \quad (15)$$

where $\rho(\tilde{A})$ is the spectral radius of $\tilde{A}$. The first constraint in Eq (15) satisfies the stability condition of the model and the second satisfies the physiological properties. $P(k)$ is the estimate of the error covariance matrix and usually $P(0)$ is selected as diagonal matrix.

$$P(k) = \frac{1}{\lambda}[P(k-1) - \frac{P(k-1)\phi(k)\phi^T(k)P(k-1)}{\lambda + \phi^T(k)P(k-1)\phi(k)}] \quad (16)$$

The forgetting factor λ in Eq (16) is the only tuning parameter adjusted by users. When $\lambda = 1$, the estimator gives equal weight to all data (infinite memory). A small value of λ gives more weight on recent observations (short memory). The estimator is slow and insensitive to disturbances for large values of λ.

3. HYPOGLYCEMIA EARLY ALARM SYSTEM

Once the unknown parameters are identified, the predictions of BGC ($\hat{\mathbf{y}}_\mathbf{p}$) can be obtained at each sampling time by using past data:

$$\hat{\mathbf{y}}_\mathbf{p} = M\left[\left(\tilde{A} - \tilde{K}\tilde{C}\right) X\,(k-1) - \tilde{K}y(k)\right] \quad (17)$$

where

$$M \triangleq \begin{bmatrix} \tilde{C} \\ \tilde{C}\tilde{A} \\ \vdots \\ \tilde{C}\tilde{A}^{N-1} \end{bmatrix} \quad (18)$$

HEA system is proposed as illustrated in the flow chart in Fig. (1). The alarm algorithm first checks the current data and if the glucose concentration is under the hypoglycemia threshold, an immediate hypoglycemia alarm is triggered. Then sleep or exercise conditions are checked via the armband (the details of the armband are provided in the result section). In case of sleep or exercise, the thresholds for signaling hypoglycemia are increased. This provides more time to compensate for potential hypoglycemia, since BGC can decrease drastically and suddenly under these states. If a GC is higher than the defined threshold, the algorithm checks for predictions of future GC to determine the need to trigger a hypoglycemia early alarm. When the n-step-ahead predicted value crosses the hypoglycemia threshold a hypoglycemia early alarm is raised.

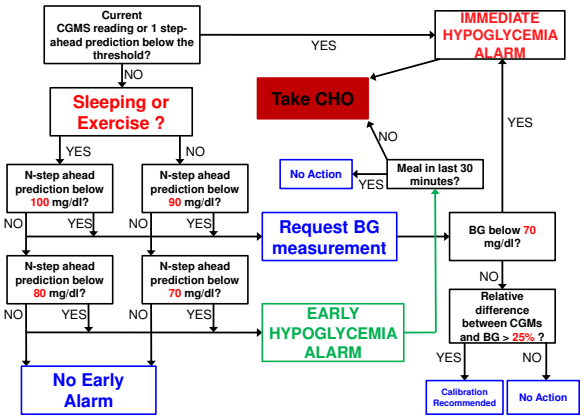

Fig. 1. Hypoglycemia early alarm flow chart for real time implementation

4. GENERALIZED PREDICTIVE CONTROL

Model-based predictive control algorithms proposed minimize a cost function for obtaining the control law. The aim is to minimize the error between the future output $\hat{y}$ and a reference trajectory r and to minimize the magnitude of the control effort u on the horizon considered:

$$\begin{aligned} J\,(N_1, N_2, N_u) = \sum_{j=N_1}^{N_2} [\hat{y}\,(k+j) - r\,(k+j)]^2 + \\ \sum_{j=1}^{N_u} w(j)[\Delta u(k+j-1)]^2 \end{aligned} \quad (19)$$

where N_1 and N_2 are the first and last time instants of the modeling horizon and N_u is the control horizon. $w(\cdot)$ is the weight for penalizing the control input. Defining

$$\begin{aligned} \hat{\mathbf{y}} &\triangleq [\,\hat{y}(k+N_1)\ \hat{y}(k+N_1+1)\ \cdots\ \hat{y}(k+N_1+N_2)\,]^T \\ \mathbf{r} &\triangleq [\,r(k+N_1)\ r(k+N_1+1)\ \cdots\ r(k+N_1+N_2\,)]^T \\ \mathbf{w} &\triangleq diag\{\,w(1)\ w(2)\ \cdots\ w(N_u)\,\} \\ \Delta\mathbf{u} &\triangleq [\,\Delta u(k)\ \Delta u(k+1)\ \cdots\ \Delta u(k+N_u-1)\,]^T \end{aligned} \quad (20)$$

the constrained control signal is calculated by minimizing

$$\begin{aligned} \mathbf{u}(k) = \min_{\mathbf{u}} \left[(\hat{\mathbf{y}} - \mathbf{r})^T(\hat{\mathbf{y}} - \mathbf{r}) + \Delta\mathbf{u}^T\mathbf{w}\Delta\mathbf{u})\right] \\ s.t.\ \mathbf{u}_{min} \leq \mathbf{u} \leq \mathbf{u}_{max} \end{aligned} \quad (21)$$

where only the first element of $\mathbf{u}(k)$ is implemented.

$$L \triangleq \begin{bmatrix} \tilde{C}\tilde{B} & 0 & \cdots & 0 \\ \tilde{C}\tilde{A}\tilde{B} & \tilde{C}\tilde{B} & \cdots & 0 \\ \vdots & \vdots & \ddots & 0 \\ \tilde{C}\tilde{A}^{N_u-1}\tilde{B} & \tilde{C}\tilde{A}^{N_u-2}\tilde{B} & \cdots & \tilde{C}\tilde{B} \\ \vdots & \vdots & \cdots & \vdots \\ \tilde{C}\tilde{A}^{N-1}\tilde{B} & \tilde{C}\tilde{A}^{N-2}\tilde{B} & \cdots & \tilde{C}\tilde{A}^{N-N_u}\tilde{B} \end{bmatrix} \quad (22)$$

where $N = N_2 - N_1$ and

$$\hat{\mathbf{y}} = LU + \hat{\mathbf{y}}_\mathbf{p} \quad (23)$$

In (23), the first part LU is called forced response while the rest of equation is called free response. Since the model in (1) is created as multi input model, U represents the future values matrix of all inputs. However, in the whole system the only control input is insulin. Thus only the first input of the model is calculated by the controller.

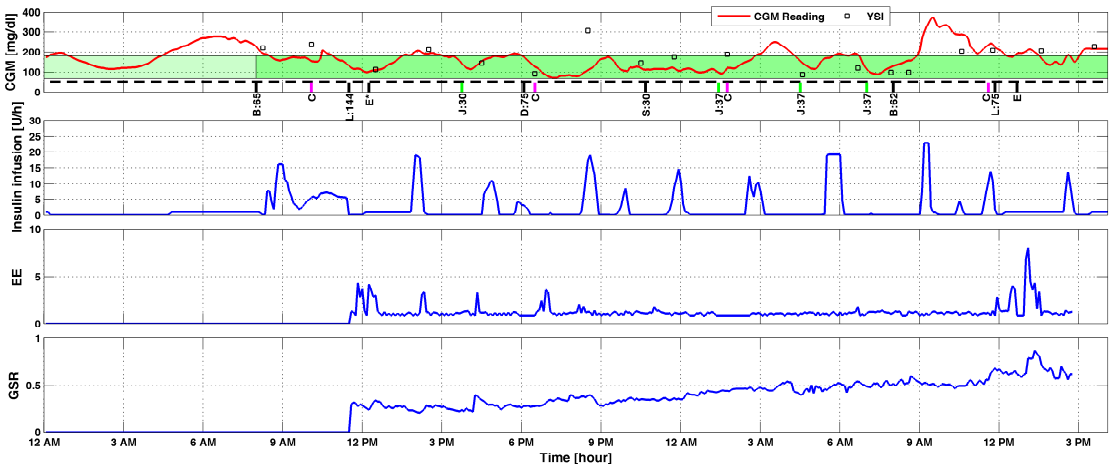

Fig. 2. Closed-loop control of a subject in CRC. Legend: Glucose concentration from CGM, infused insulin rate (Ins), energy expenditure (EE) and galvanic skin response (GSR). B: breakfast, L: lunch, D: dinner, S: snack, E: exercise, C: calibration. The green band indicates the normal range of blood glucose concentration. The darker green section indicates the closed-loop duration. The black dashed line shows hypoglycemia threshold. Vertical bars; black: regular meal, snack or exercise, green: early alarm-based meal or snack, magenta: calibration.

The predictions of the other input signals have to be implemented externally. Each input signal is used in an ARMA model to calculate their predicted values:

$$A_i(q^{-1})y_i(k) = C_i(q^{-1})\epsilon_i(k) \tag{24}$$

where $y_i(k)$ represents inputs of (1) except the first input. The predictions of inputs $i = 2, \cdots, m$ yield:

$$\hat{\mathbf{y}}_\mathbf{i} \triangleq \left[\, \hat{y}_i(k+N_1-d_i) \;\; \hat{y}_i(k+N_1+1-d_i) \;\; \cdots \;\; \hat{y}_i(k+N_1+N_2-d_i) \,\right]^T \tag{25}$$

$$\hat{\mathbf{y}}_\mathbf{i} = M_i \left[\left(\tilde{A}_i - \tilde{K}_i \tilde{C}_i \right) X_i\,(k-1) - \tilde{K}_i y_i(k) \right] \tag{26}$$

where M_i, $\tilde{A}_i$, $\tilde{K}_i$, $\tilde{C}_i$, and $\tilde{X}_i(k-1)$ can be calculated by using (5) to (23) based on the model in (24). Then,

$$U = \mathbf{u} + \hat{\mathbf{y}}_\mathbf{2} + \cdots + \hat{\mathbf{y}}_\mathbf{m} \tag{27}$$

5. RESULTS

Subjects were recruited from the University of Chicago Medical Center, Kovler Diabetes Center and were scheduled for a visit at the University of Chicago General Clinical Research Center (GCRC). Subjects were young adults aged 18-35 years with T1D. All subjects used insulin pump therapy, were healthy and physically active. Each visit was approximately 70 hours long and the first day was used for sensor calibration and open-loop operation under conditions that the subjects will face the following two days during the closed-loop experiment. The subject's own insulin type and pump were used in the experiments. Subjects were provided a total of 8 meals and snacks during the 2 days of the closed-loop experiment. Data were continuously collected every 10 minutes from the subjects. CGM readings were manually entered to the computer every ten minutes and SenseWear signals were recorded wirelessly. Every 10 minutes insulin infusion rates were computed by the controller and reviewed by a medical expert. Upon approval, the computed insulin infusion rates were entered manually to the subject's insulin pump.

Two Guardian® REAL-time CGM (Medtronics, Northride, CA) were used to collect the glucose concentration information. The Guardian® REAL-time CGM system measures glucose in the interstitial tissue and displays the GC every 5 minutes. The SenseWear Pro3 armband (BodyMedia Inc, Pittsburgh, PA) worn on the dominant upper arm over the triceps muscle collects metabolic and physical activity data. Each subject participated in a 20-minute exercise bout (treadmill running) of moderate-to-intense intensity before or after lunch. The subjects ran using a ramped protocol where the speed (miles per hour [mph]) and the incline (%) of the treadmill were gradually increased until the exercise session ended. Overall, the subjects exercised 85±8.3 % (mean and standard deviation) of their age-predicted heart rate of 220-age (American College of Sports Medicine, 2010) (range: 70-97%).

Every two hours and before meals, BGC was measured using a blood glucose meter or YSI (Yellow Springs Instrument (YSI) 2300 STAT; Yellow Springs, Ohio). The meter BGC value was entered to CGM devices for calibration, if there was a significant difference (25% $\leq$ relative difference) between the CGM reading and the meter measurements and glucose values were stable.

Closed-loop control was performed for 32 hours for each subject. Breakfast, lunch, dinner and a late night snack were provided based on protocol. Additional snacks were provided whenever requested by the subjects. No limitation on food or snack was imposed. All subjects performed a treadmill exercise after or before lunch. The exercise intensity was adjusted based on target heart rate and the upper exercise tolerance limit of the subjects. Each subject was free to stop the exercise at any time.

The integrated multivariable HEA and GC control system recommends insulin infusion rates for high GC values and triggers hypoglycemia warnings when low GC values are predicted. Sleep or exercise states are noted prior to deciding on the final insulin infusion rate. The system requires a confirmatory finger-stick (or YSI) measurement when hypoglycemia is detected. If the finger-stick value is less than the threshold, an early alarm is triggered and treatment with a 15 g carbohydrate (CHO) snack is suggested (Fig. 1). However, the subject does not have to eat the snack if a meal was consumed within the last 30 minutes as the amount of CHO ingested during the

meal should be sufficient to prevent hypoglycemia. Once the snack is eaten, a flag is lifted inside the algorithm to prevent the continuous alarm; this will prevent snack induced hyperglycemia. When the predicted and confirmatory finger-stick value are above the GC thresholds, the flag is brought down and the system is prepared to give a new early alarm when future episodes of hypoglycemia are predicted.

Fig. (2) shows the closed-loop results for one subject. The experiment began at 0815 hours with a confirmatory YSI measurement. The subject ate breakfast, with 65 g CHO at 0820 hours. The CGM and insulin pump were calibrated based on a finger-stick meter value at 1010 hours because the difference between the CGM and other readings was high (CGM: 153 mg/dl, YSI: 238 mg/dl). The subject had 144 grams of CHO at lunch around 1130 hours. Based on the protocol, the subject was supposed to have a high-intensity treadmill exercise after lunch. But the subject preferred to have a walking exercise for 30 minutes (E* in Fig. 2). Once the exercise started, EE measurements informed the controller about the exercise, which subsequently suggested less aggressive insulin dosing to prevent post-exercise hypoglycemia. The HEA system triggered a low GC prediction alarm at 1545 hours, and two glasses of orange juices (30 g CHO) were consumed by the subject. 75 g CHO was provided at dinner at 1805 hours. At 0145, 0432, and 0630 hours, the HEA triggered alarms, and juice (37 g CHO) was provided each time. On the second day, the protocol-based high-intensity treadmill exercise was performed after lunch. Overall, CGM values stayed inside the normal range 66% of the time, between 180-250 mg/dl 29% of the time and above 250 mg/dl 5% of the time during the closed-loop study. No hypoglycemia occurred. Whenever a hypoglycemia limit was approached based on HEA predictions, CHO was provided and GC rose. Physical activity data from 0000 to 1100 hours were lost because of technical problems.

Fig. (3) shows the results of a 24 hours period of an open-loop experiment where insulin amounts were calculated by the subject. The subject did not infuse insulin for a snack around 0020 hours and breakfast around 1000 hours. This happens either because subjects think there is no need for infusion or forget infusing insulin. Around 1630 hours, the subject had exercise and subsequently hypoglycemia occured. Additional snacks were eaten, but it took time to rescue GC to normal range, since the snacks were consumed at a time when the subject was already in hypoglycemia. After dinner, the subject infused a bolus at 2020 hours and a correction bolus around 2220 hours. All bolus amounts were identical even though different amounts of food were consumed.

Table 1. Performance Comparison. OP: open-loop, MCL: multivariable closed-loop, IMCL: integrated multivariable closed-loop

	Mean±SD	70-180 mg/dl (%)	Hypoglycemia
OP (n=2)	209 ± 102.8	34.9	Severe
MCL (n=2)	166 ± 56.1	70.8	Mild
IMCL (n=2)	170 ± 60.5	63	None

The results of six experiments are summarized in Table 1. The mean value of glucose for open-loop experiments is higher than other two groups as well as severe hypoglycemia episodes (GC$\approx$ 40 mg/dl) were seen at multiple time points during the open-loop experiments. The probability of hypoglycemia is decreased with our multivariable adaptive control algorithm and eliminated with the proposed integrated system.

6. DISCUSSION

A multivariable AP control system that integrated an HEA was tested as an AP system could prevent hyperglycemia after meals and alert for predicted hypoglycemia after exercise and during sleep. Clinical experiments showed that this system alarmed when hypoglycemia was predicted so that preventive action could be taken in a timely manner.

As it is seen in Fig. (3) a subject may not always calculate the appropriate dose of insulin or may even forget to infuse insulin. This usually causes hyperglycemia. Hypoglycemia may be caused by incorrect boluses and exercise. The proposed AP prevented hypoglycemia in our clinical study.

The probability of hypoglycemia is minimized based on prediction of GC. A snack is suggested to be consumed at least 25 minutes before the predicted hypoglycemic event which can prevent most of hypoglycemia. Even though patient does not attend the suggestion, the controller stops insulin infusion which prevents further decrease in glucose levels.

7. CONCLUSIONS

A HEA system integrated into an AP controller was successful in glucose regulation in patients with type 1 diabetes and in generating early alarms when hypoglycemia was predicted. Post-exercise and sleep-induced hypoglycemia did not occur when such a system was used. The integrated system is fully adaptive and does not require any meal or physical activity announcements.

ACKNOWLEDGEMENTS

Funding from the National Institutes of Health NIDDK R01 DK 085611 is gratefully acknowledged.

REFERENCES

American College of Sports Medicine (2010). *ACSM's resource manual for guidelines for exercise testing and prescription*. Wolters Kluwer Health/Lippincott Williams & Wilkins.

American Diabetes Association (2013). Economic costs of diabetes in the us in 2012. *Diabetes Care*, 36(4), 1033–1046.

Bequette, B.W. (2005). A critical assessment of algorithms and challenges in the development of a closed-loop artificial pancreas. *Diabetes Technol Ther*, 7(1), 28–47. doi:10.1089/dia.2005.7.28.

Breton, M., Farret, A., Bruttomesso, D., Anderson, S., Magni, L., Patek, S., Dalla Man, C., Place, J., Demartini, S., Del Favero, S., et al. (2012). Fully Integrated Artificial Pancreas in Type 1 Diabetes Modular Closed-Loop Glucose Control Maintains Near Normoglycemia. *Diabetes*, 61(9), 2230–2237.

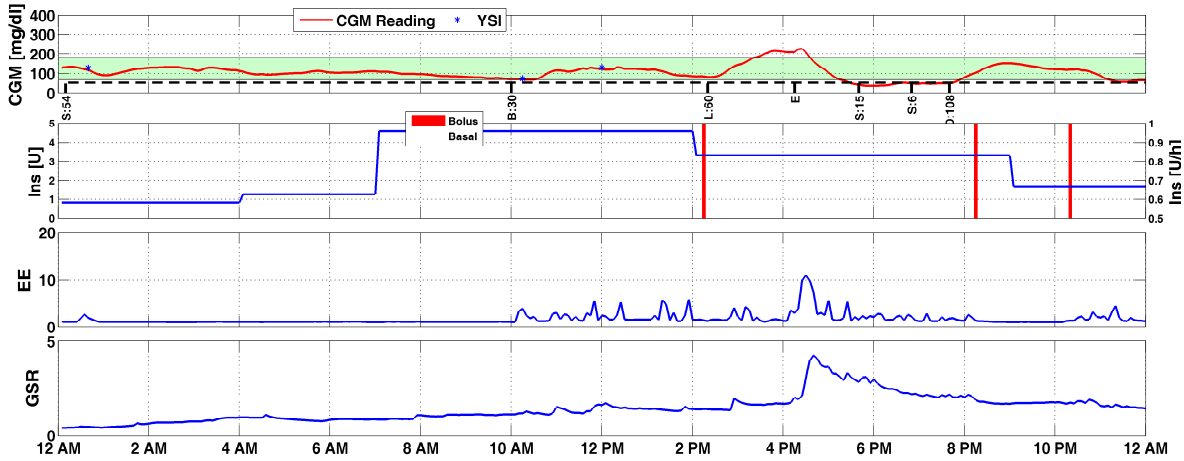

Fig. 3. Open-loop GC regulation by a subject at CRC. Legend: refer to Fig. 2.

Bruttomesso, D., Farret, A., Costa, S., Marescotti, M.C., Vettore, M., Avogaro, A., Tiengo, A., Dalla Man, C., Place, J., Facchinetti, A., Guerra, S., Magni, L., De Nicolao, G., Cobelli, C., Renard, E., and Maran, A. (2009). Closed-loop artificial pancreas using subcutaneous glucose sensing and insulin delivery and a model predictive control algorithm: preliminary studies in Padova and Montpellier. *Journal of Diabetes Science and Technology*, 3(5), 1014–1021.

Buckingham, B., Cobry, E., Clinton, P., Gage, V., Caswell, K., Kunselman, E., Cameron, F., and Chase, H.P. (2009). Preventing hypoglycemia using predictive alarm algorithms and insulin pump suspension. *Diabetes Technology & Therapeutics*, 11(2), 93–97. doi: 10.1089/dia.2008.0032.

Clarke, W.L., Anderson, S., Breton, M., Patek, S., Kashmer, L., and Kovatchev, B. (2009). Closed-loop artificial pancreas using subcutaneous glucose sensing and insulin delivery and a model predictive control algorithm: the Virginia experience. *Journal of Diabetes Science and Technology*, 3(5), 1031–1038.

El-Khatib, F.H., Russell, S.J., Nathan, D.M., Sutherlin, R.G., and Damiano, E.R. (2010). A bihormonal closed-loop artificial pancreas for type 1 diabetes. *Sci Transl Med*, 2(27), 27ra27. doi:10.1126/scitranslmed.3000619.

Elleri, D., Allen, J., Nodale, M., Wilinska, M., Acerini, C., Dunger, D., and Hovorka, R. (2010). Suspended insulin infusion during overnight closed-loop glucose control in children and adolescents with type 1 diabetes. *Diabetic Medicine*, 27(4), 480–484.

Elleri, D., Allen, J.M., Kumareswaran, K., Leelarathna, L., Nodale, M., Caldwell, K., Cheng, P., Kollman, C., Haidar, A., Murphy, H.R., et al. (2013). Closed-loop basal insulin delivery over 36 hours in adolescents with type 1 diabetes randomized clinical trial. *Diabetes care*, 36(4), 838–844.

Eren-Oruklu, M., Cinar, A., Rollins, D.K., and Quinn, L. (2012). Adaptive system identification for estimating future glucose concentrations and hypoglycemia alarms. *Automatica*, 48(8), 1892–1897.

Ruiz, J., Sherr, J., Cengiz, E., Carria, L., Roy, A., Voskanyan, G., Tamborlane, W., Weinzimer, S., et al. (2012). Effect of insulin feedback on closed-loop glucose control: a crossover study. *Journal of diabetes science and technology*, 6(5), 1123–1130.

Schaller, H., Schaupp, L., Bodenlenz, M., Wilinska, M., Chassin, L., Wach, P., Vering, T., Hovorka, R., and Pieber, T. (2006). On-line adaptive algorithm with glucose prediction capacity for subcutaneous closed loop control of glucose: evaluation under fasting conditions in patients with type 1 diabetes. *Diabetic medicine*, 23(1), 90–93.

Sparacino, G., Zanderigo, F., Corazza, S., Maran, A., Facchinetti, A., and Cobelli, C. (2007). Glucose concentration can be predicted ahead in time from continuous glucose monitoring sensor time-series. *Biomedical Engineering, IEEE Transactions on*, 54(5), 931–937. doi: 10.1109/TBME.2006.889774.

Steil, G.M., Rebrin, K., Darwin, C., Hariri, F., and Saad, M.F. (2006). Feasibility of automating insulin delivery for the treatment of type 1 diabetes. *Diabetes*, 55(12), 3344–3350. doi:10.2337/db06-0419.

Steil, G., Palerm, C., Kurtz, N., Voskanyan, G., Roy, A., Paz, S., and Kandeel, F. (2011). The effect of insulin feedback on closed loop glucose control. *Journal of Clinical Endocrinology & Metabolism*, 96(5), 1402–1408.

Turksoy, K., Bayrak, E.S., Quinn, L., Littlejohn, E., and Cinar, A. (2013a). Multivariable Adaptive Closed-Loop Control of an Artificial Pancreas without Meal and Activity Announcement. *Diabetes Technology & Therapeutics*, 15(5), 386–400. DOI: 10.1089/dia.2012.0283.

Turksoy, K., Bayrak, E.S., Quinn, L., Littlejohn, E., Rollins, D.K., and Cinar, A. (2013b). Hypoglycemia Early Alarm Systems Based On Multivariable Models. *Industrial Eng. Chemical Research*, 52(35), 12329–12336. doi:10.1021/ie3034015.

Ward, W., Castle, J., and El Youssef, J. (2011). Safe glycemic management during closed-loop treatment of type 1 diabetes: the role of glucagon, use of multiple sensors, and compensation for stress hyperglycemia. *Journal of Diabetes Science and Technology*, 5(6), 1373–1380.

Weinzimer, S.A., Steil, G.M., Swan, K.L., Dziura, J., Kurtz, N., and Tamborlane, W.V. (2008). Fully automated closed-loop insulin delivery versus semiautomated hybrid control in pediatric patients with type 1 diabetes using an artificial pancreas. *Diabetes Care*, 31(5), 934–939. doi:10.2337/dc07-1967.